Supplementary files for:

Two-stage electro-mechanical coupling of a K$_V$ channel in voltage-dependent activation

Panpan Hou, Po Wei Kang, Audrey Deyawe Kongmeneck, Nien-Du Yang,

Yongfeng Liu, Jingyi Shi, Xianjin Xu, Kelli McFarland White, Mark A. Zaydman, Marina A.

Kasimova, Guiscard Seebohm, Ling Zhong, Xiaoqin Zou, Mounir Tarek*, and Jianmin Cui*

*To whom correspondence should be addressed. E-mail: jcui@wustl.edu (J.C.) or

mounir.tarek@univ-lorraine.fr (M.T.)

This PDF File Includes:

Supplementary Table 1

Supplementary Figures. 1 to 7

**Supplementary Table 1. All primer sequences used in this study.**

Mutations	Primer sequences
C214A	pB: cttggaTcccacCGCgaggaccacca pC: cGCGgtgggAtccaaggggcaggtg
G219C	pB: cctgaCacttggaTcccacCGC pC: ggAtccaagtGtcaggtgtttgccacg
C331A	pB: gacagagaaTGCggaggcgatggtcttc pC: ctccGCAttctctgtctttgccatc
E160R	pB: cgatTCTcatccagaagagagt pC: ctcttctggatgAGAatcgtgctggtggtgttct
R231E	pB: caggaaTTCgatgcccctgatggc pC: gggcatcGAAttcctgcagatcctgag
R237E	pB: gcatcTCcaggatctgcaggaag pC: cagatcctgGAgatgctacacgtcgac
F127A	pB: gaagacggcgGCAtggtaaacgaagcatttc pC: caTGCcgccgtcttcctcatc
K183N	pB: cacgtaAttgctgcggcagcc pC: ccgcagcaaTtacgtgggcctctgg
R190Q	pB: gcagcTgcccccagaggcc pC: ctgggggcAgctgcgctttgccc
F193A	pB: cgTgcaGCgcgcagccgcccc pC: ctgcgcGCtgcAcggaagcccatttcc
R195A	pB: ggcttAGCggcaaagcgcagccg pC: gctttgccGCTaagcccatttccatcatc
K196E	pB: ctgcgctttgcccggGagcccatttc pC: ccggGagcccatttccatcatc
P197A	pB: ggaaatTGCcttccgggcaaagcg pC: ccggaagGCAatttccatcatcgacctc
R237W	pB: gcatccAcagTatctgcaggaagcgg pC: cagatActgTggatgctacacgtcg
Q244W	pB: cctccccaccggtcgacgtgtagc pC: gaccggtggggaggcacctggag
G245W	pB:ccaggtcccccactggcggtcgacgtg pC:cagtggggggacctggaggctcct
G246W	pB: ccaggtccaaccctggcggtcgac pC:cagggttggacctggaggctcctg
T247W	pB: gagtctccaccagcctccctggcggtc pC: ggctggtggagactcctgggctccgtg
W248R	pB: cctccGggtgcctccctggc pC: gaggcaccCggaggctcctgggc
R249W	pB: gagccAccaCgtgcctccctggcg pC: ggcacGtggTggctcctgggctcc
L250W	pB: gagccGagCCAcctccaggtgcctc pC: gaggTGGctCggctccgtggtcttc

L251A	pB: cggaTcccGCgagcctccaggtgcc
	pC: gctcGCgggAtccgtggtcttcatcc
G252W	pB: gaccacTgaCcAcaggagcctccaggtg
	pC: cctgTgGtcAgtggtcttcatccaccg
S253W	pB: gaccacCCagcccaggagcctcc
	pC: gggctGGgtggtcttcatccacc
V254M	pB: gaagaccaTggagcccaggagcc
	pC: ggctccAtggtcttcatccaccg
V255W	pB: gatgaaCCAcacggagcccaggag
	pC: ctccgtgTGGttcatccaccgccagg
F256A	pB: gtggatgGCgaccacggagcccag
	pC: gtggtcGCcatccaccgccagg
I257W	pB: gcggtgCCAAaagaccacggagccc
	pC: ggtcttTTGGcaccgccaggagctg
H258W	pB: ctggcgCCAgatgaagaccacggag
	pC: cttcatcTGGcgccaggagctgataac
R259W	pB: cagctcctgCcAgtggatgaagaccacgg
	pC: cacTgGcaggagctgataaccac
Q260W	pB: gctccCACcggtggatgaagaccac
	pC: ccaccgGTGggagctgataaccacc
E261K	pB: gttatAagctTctggcggtggatgaag
	pC: cgccagAagctTataaccaccctgtacatc
L262A	pB: ggtggtAatTGCctcctggcggtggatg
	pC: ggagGCAatTaccaccctgtacatcg
I263A	pB: ggtggttGCcagctcctggcggtg
	pC: gagctgGCaaccaccctgtacatc
T264A	pB: cagTgtggCtatcagctcctggcg
	pC: ctgataGccacActgtacatcg
T265A	pB: gtacagAgCggttatcagctcctg
	pC: gataaccGcTctgtacatcggcttc
L266A	pB: GATAACCACCGCCTACATCG
	pC: CGATGTAGGCGGTGGTTATC
Y267A	pB: ccgatAGCcagggtggttatcagc
	pC: caccctgGCTatcggcttcctgggcc
I268W	pB: gaagccCCAgtacagggtggttatcag
	pC: cctgtacTGGggcttcctgggcctc
G269A	pB: CTGTACATCGCCTTCCTGGGCCT
	pC: AGGCCCAGGAAGGCGATGTACAG
F270A	pB: GTACATCGGCGCCCTGGGCCTC
	pC: GAGGCCCAGGGCGCCGATGTAC
L271E	pB: gatgaggccTTCgaagccgatgtacagg
	pC: cttcGAAggcctcatcttctcc
G272A	pB: CTTCCTGGCCCTCATCTTCT
	pC: AGAAGATGAGGGCCAGGAAG
L273F	pB: gaagatgaATcccaggaagccgatg
	pC: cctgggATtcatcttctcctcgtac

|	
I274A	pB: TGGGCCTCGCCTTCTCGAGCTA pC: TAGCTCGAGAAGGCGAGGCCCA
F275A	pB: GCCTCATCGCCTCGAGCTA pC: TAGCTCGAGGCGATGAGGC
F335A	pB: CTTCTCTGTCGCTGCCATCTCC pC: CTTCTCTGTCGCTGCCATCTCC
A336G	pB: gaaggaAatTCcaaagacagagaagcag pC: gtctttgGAatTtccttctttgcgctcc
I337A	pB: CTGTCTTTGCCGCCTCCTTCTTTGC pC: GCAAAGAAGGAGGCGGCAAAGACAG
S338F	pB: gaagAATatTgcaaagacagagaag pC: gtctttgcAatATTcttctttgcgctccc
F339S	pB: gcaaaACTggagatggcaaagacag pC: ccatctccAGTtttgcgctcccagcg
F340A	pB: GCCATCTCCTTCGCTGCGCTCCCA pC: TGGGAGCGCAGCGAAGGAGATGGC
A341V	pB: gggagcAcaaagaaggagatggc pC: ccttctttgTgctcccagcgggg
L342A	pB: CTTCTTTGCGGCCCCAGCG pC: CGCTGGGGCCGCAAAGAAG
P343A	pB: ccgcGgCgagcgcaaagaaggag pC: gcgctcGcCgcggggattcttggc
A344V	pB: gaatccccActgggagcgcaaagaag pC: ctcccagTgggggattcttggctcg
G345A	pB: gccaagaatcGccgctgggagcgc pC: gcggCgattcttggctcggg
I346A	pB: gagccaagGGCcccccgctgggagcgc pC: gggGCCcttggctcggggtttg
L347A	pB: gagccaGCaatccccgctgggagc pC: ggggattGCtggctcggggtttgcc
G348A	pB: ccgaCGcaagaatccccgctg pC: ggattcttgCGtcggggtttgccctg
S349A	pB: gcaaaccccgCgccaagaatccccgc pC: ggcGcggggtttgccctg
G350A	pB: ggcaaacGccgagccaagaatcc pC: gctcggCgtttgccctgaaggtg
F351A	pB: ggcaGCGcccgagccaagaatcc pC: gctcgggCGCtgccctgaaggtgcag
A352C	pB: GATCCGGGTTTTGCCTGAAGGTGCAG pC: CTGCACCTTCAGGCAAAACCCGGATC
L353K	pB: ccttcTTggcaaaccccgagc pC: gggtttgccAAgaaggtgcagcagaag
K354A	pB: ctgcacGGCcagggcaaaccccg pC: ccctgGCCgtgcagcagaagcag
V355W	pB: gggtttgccctgaagTGgcagc pC: gggtttgccctgaagTGgcagc

Q356A	pB: GTTTGCCCTGAAGGTGGCGCAGAAGCAG pC: CTGCTTCTGCGCCACCTTCAGGGCAAAC
Q357A	pB: GAAGGTGCAGGCGAAGCAGAGGCAGA pC: TCTGCCTCTGCTTCGCCTGCACCTTC
K358A	pB: GTGCAGCAGGCGCAGAGGCAGAAGCAC pC: GTGCTTCTGCCTCTGCGCCTGCTGCAC
Q359A	pB: GTGCAGCAGAAGGCGAGGCAGAAGCAC pC: GTGCTTCTGCCTCGCCTTCTGCTGCAC
R360A	pB: CAGCAGAAGCAGGCGCAGAAGCACTTC pC: GAAGTGCTTCTGCGCCTGCTTCTGCTG
M238W	pB: gacgtgCagcCAcctcaggatctgcagg pC: gaggTGgctGcacgtcgaccgccag
E160R/ R237E/ M238W	Use E160R/R237E as template M238W-pB: gacgtgCagcCAcTCcaggatctgcagg M238W-pC: GAgTGgctGcacgtcgaccgccag
L239W	pB: cgacgtgCCAcatcctcaggatctgc pC: ggatgTGGcacgtcgaccgccag
E160R/ R237E/ L239W	Use E160R/R237E as template L239W-pB: gacgtgCCAcatcTCcaggatctgc L239W-pC: GAgatgTGGcacgtcgaccgccag
D242W	pB: gcgCCAgacgtgtagcatcctc pC: ctacacgtcTGGcgccagggaggcac
R243W	pB: ccctgCcAgtcgacgtgtagcatc pC: gtcgacTgGcagggaggcacctgg
I268A	pB: caggaaTccgGCgtacaggtggttatcag pC: gtacGCcggAttcctgggcctcatcttc
L251F	pB: gagccGaAgagcctccaggtgcc pC: gaggctcTtCggctccgtggtcttc
F339L	pB: cgcGaaGaGggagatggcaaagacag pC: catctccCtCttCgcgctcccagcggg

Supplementary Figures
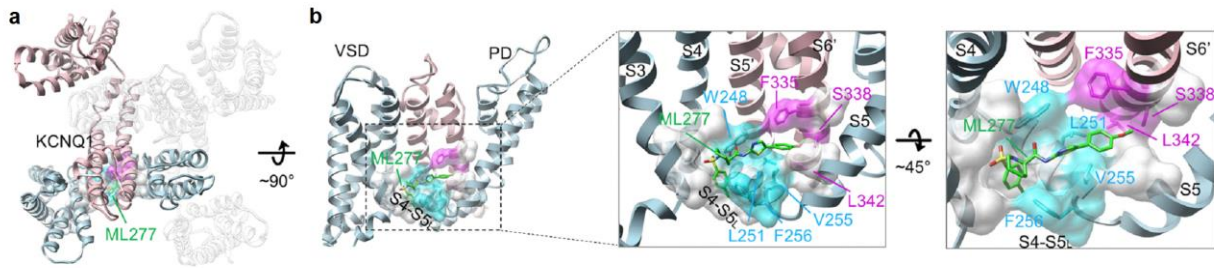
Supplementary Fig. 1, Molecular docking results of ML277 onto KCNQ1 channel.
(a) Residues interacting with ML277 based on molecular docking and experimental results. Top view of the binding mode of ML277 (green) at the homology model of hK$_V$7.1 (see Methods). Two neighboring subunits (light red and light blue) are highlighted. **(b)** Side view of the binding mode of ML277. Only two neighboring subunits (light red and light blue) are shown for clarity. Right panels, detailed structure of the ML277 (green) binding at the S4-S5L/pore interface. Interacting residues that consistent with mutagenesis results shown in cyan (S4-S5L) and magenta (pore).
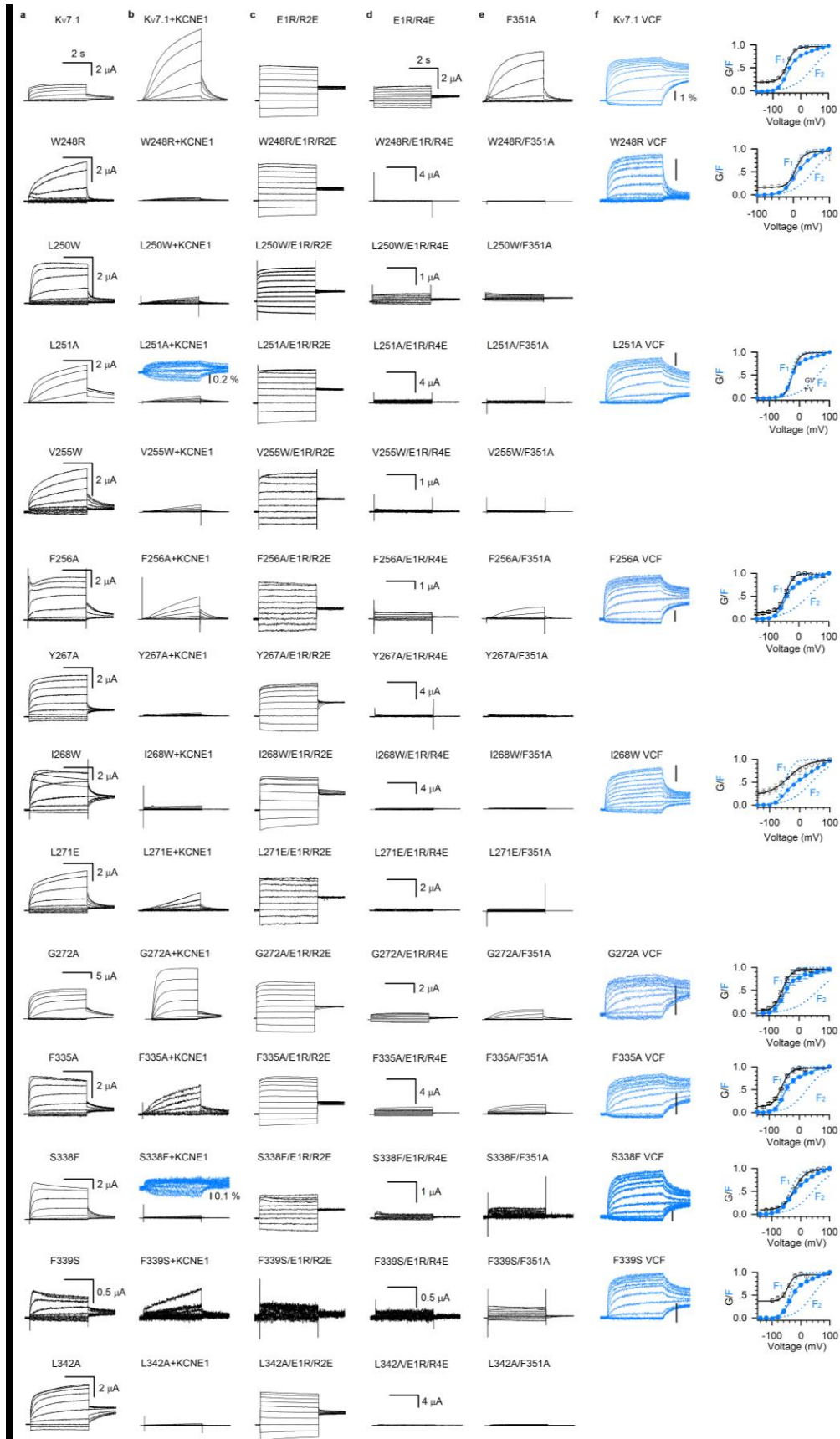
Supplementary Fig. 2. Dataset for functional validations of AO state E-M coupling residues identified by the ML277 screen.

(a-b) Currents of WT and mutant $K_V7.1$ with and without KCNE1. Currents are shown in the same scale. VCF experiments was performed on S338F+KCNE1 and L251A+KCNE1, indicating membrane expression and VSD function. **(c-e)** Currents of WT and mutant $K_V7.1$ on top of the IO background E1R/R2E, the AO background E1R/R4E and F351A. Currents are shown in the same scale. **(f)** VCF results of WT and eight mutations in $K_V7.1^*$. n ≥ 3. Source data are provided as a Source Data file.
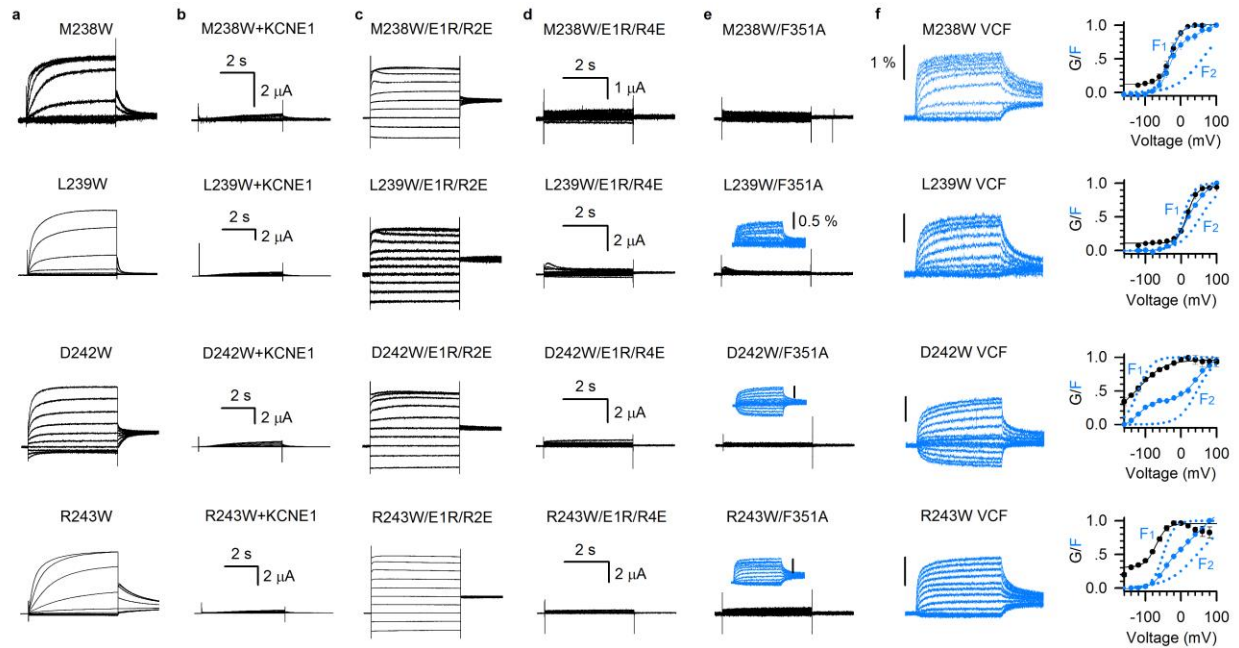
Supplementary Fig. 3. Dataset for functional validations of S4c residues critical for AO state E-M coupling.

(**a-b**) Currents of S4c mutations with and without KCNE1. Currents are shown in the same scale. (**c-e**) Currents of the S4c mutations on top of the IO background E1R/R2E, the AO background E1R/R4E and F351A. Currents are shown in the same scale. VCF results (three out of four) are shown in blue. (**f**) VCF results of the four mutations in S4c in $K_V7.1^*$. n ≥ 3. Source data are provided as a Source Data file.
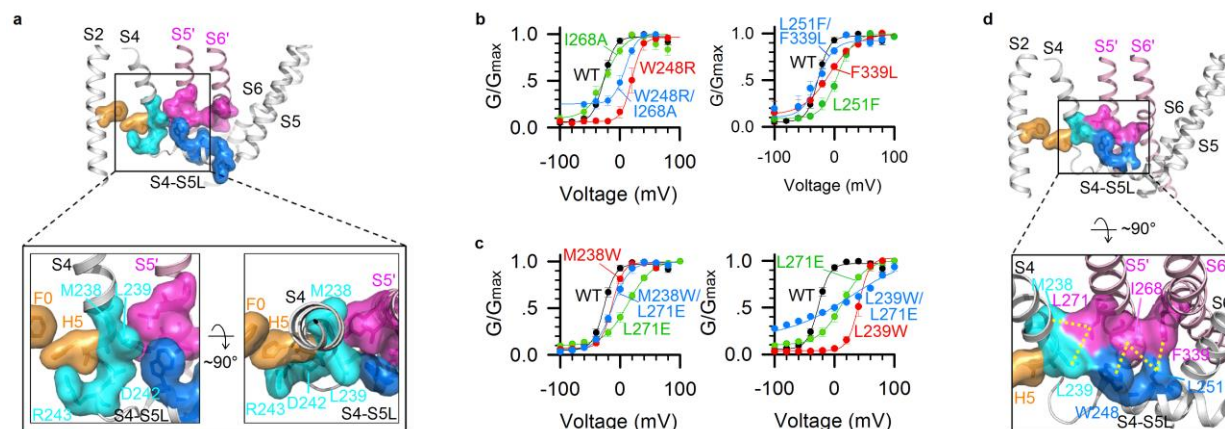
Supplementary Fig. 4. Double mutant cycle analysis.

(a) Mapping the key residues on to the Kv7.1 cryoEM structure, the VSD of which is at the activated state. Cyan, S4c residues (M238, L239, D242, and R243); Orange, F0 and H5 in the charge transfer center; Blue, S4-S5L residues; Pink, pore residues. Lower panels, detailed structure of the key residues. (b-c) Double mutant cycle analysis of the interactions at S4-S5L/pore interface: W248 and I268 (ΔΔG= 1.4 kcal/mol) and L251 and F339 (ΔΔG= 2.7 kcal/mol), as well as the S4c/S5 interface: M238 and L271 (ΔΔG= 1.7 kcal/mol) and L239 and L271 (ΔΔG= 4.4 kcal/mol). G–V relations from WT and mutations are fitted with Boltzmann equation. n ≥ 3. (d) Mapping the interactions M238/L271 and L239/L271 at the S4c/S5 interface, and W248/I268, L251/I268, and L251/F339 at the S4-S5L/pore interface. Color code is the same as in a, and yellow dashed lines indicate the interactions.

a

b

State-dependent salt bridges in Kv7.1 models				
Salt bridge	Number of subunits (over 4)			
	RC	IO	AO	AC
E1/R1	3	0	0	0
E2/R2	3	0	0	0
E1/R2	1	4	0	0
E2/R4	0	3	0	0
E1/R4	0	0	4	4

c

d

e

Neighbor residues in Kv7.1 models				
Residue pairs	Number of subunits (over 4)			
	RC	IO	AO	AC
T144/S298	4	3	4	4
T144/Y299	4	4	4	4
T144/A300	4	3	4	4
F232/F279	3	4	4	4
L250/L353	4	4	4	0
V254/L353	4	4	4	4
H258/L353	4	4	4	4

f

g

h
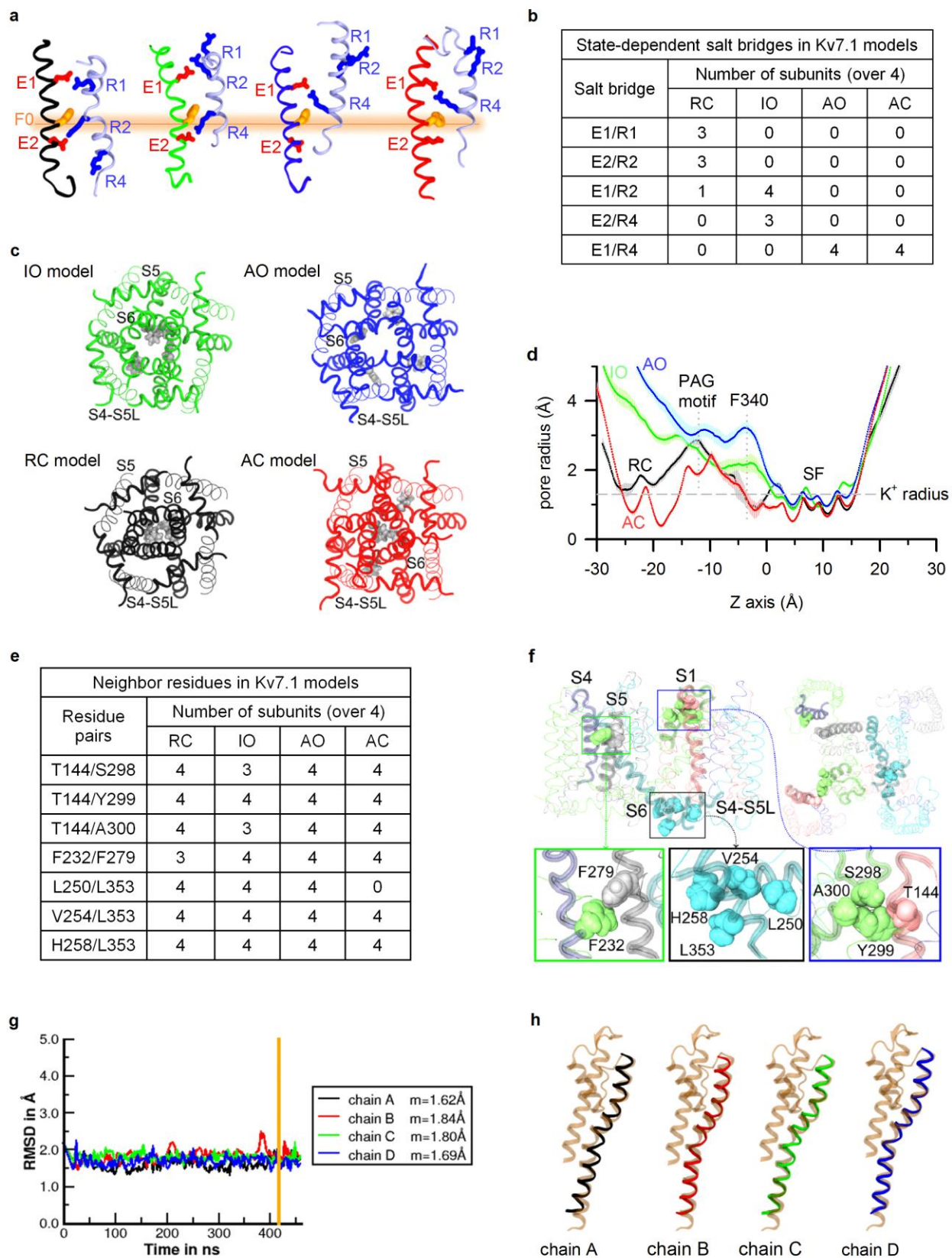
Supplementary Fig. 5. Structural validation of the MD trajectories obtained for $K_V7.1$ models.
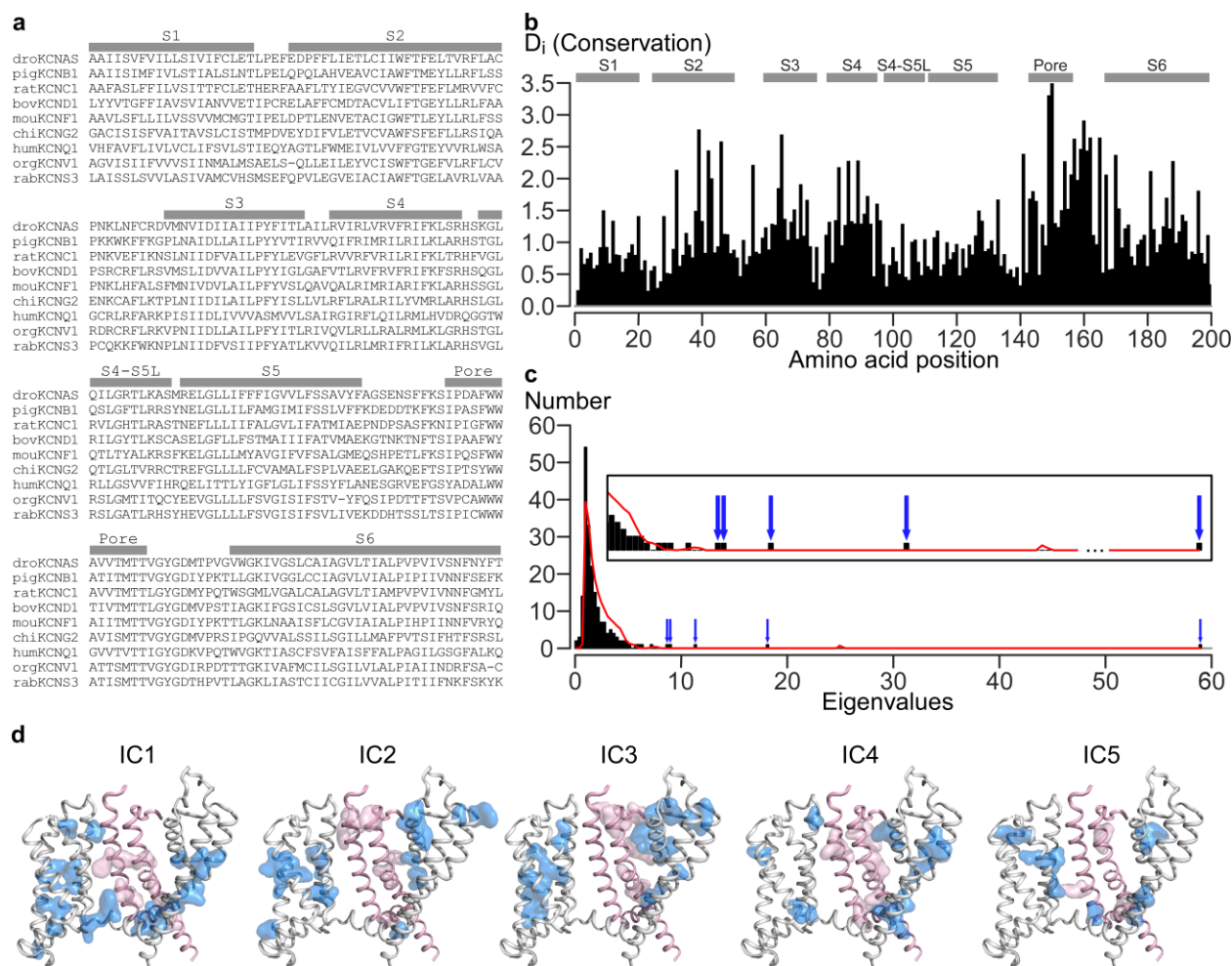
(a) State-dependent $K_V7.1$ VSD salt-bridges[1-4]. Representation of S2 (in black, green, blue and red) and S4 (in blue) segments in $K_V7.1$ RC, IO, AO and AC models, respectively. S4 gating charges are represented in blue sticks, while its S2 countercharges are represented in red sticks. The hydrophobic plug F167 (F0) is represented in orange sticks. (b) Summary table of state-dependent $K_V7.1$ VSD salt-bridges in the subunits of $K_V7.1$ models. (c) Intracellular view of S4-S5L and PD segments in $K_V7.1$ IO (top, left), AO (top, right), RC (bottom, left) and AC (bottom, right) models. The gray spheres are sidechains of F340. (d) Average pore radii of the conduction pathways of $K_V7.1$ models. Standard deviations are represented by black, green, blue and red horizontal bars for the MD trajectories obtained from RC, IO, AO and AC models, respectively. (e) Summary table of state-dependent KCNQ1 neighbor residues pairs identified by cysteine scanning studies and previous double mutant cycle analysis in the subunits of KCNQ1 RC, IO, AO and AC models involving T144 [5], F232 [6], and L353 [7]. In this analysis we calculated the distance between Cβ atoms of the residue pairs with a cut-off of 13 Å to determine if these residues are prone to interact when mutated into Cys. (f) Interacting pairs of KCNQ1 neighbor residues. In the upper panel, the side view (left) and the extracellular view (right) of the seven pairs of neighbor residues in the KCNQ1 IO model are shown. The transmembrane segments (in cartoon) bearing the residues of interest are highlighted in transparent colors. In the lower panel, the zoomed views of IO state specific interaction in IO model (left), RC state specific interactions in RC model (middle), and of AO state specific residue pairs in AO model (right) are displayed. (g-h) Comparison of the pore domain of $K_V7.1$ RC model with KCNQ1$_{EM}$ structure. (g) The graph project the root-mean-square deviation (RMSD) of the pore domain segments of $K_V7.1$ RC model with respect to KCNQ1$_{EM}$ structure throughout its MD simulation time (in ns). Average RMSD values are displayed for each subunit (labeled chain A, B, C, D). The orange vertical line represents the simulation time at which the pictures displayed in (h). (h) A cartoon representation of the structural alignment of the S6 segment of KCNQ1$_{EM}$ structure (in transparent orange) with those of $K_V7.1$ (top) RC subunits, each captured at ~420 ns. Each subunit is represented in solid black, red, green and blue cartoon, respectively. Source data are provided in Source Data file.
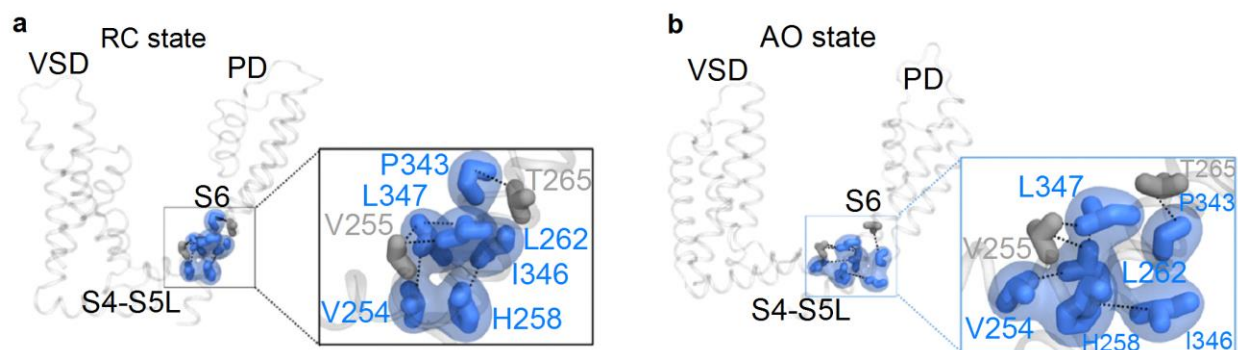
Supplementary Fig. 6. Possible intra-subunit interactions at the classical E-M coupling region in RC and AO states.

(a-b) Representations of the IO and AO state models of a $K_V7.1$ subunit. Inset: enlarged structures of the boxed area. Blue, residues identified as important for E-M coupling in experiments (Fig. 1c-g); grey: V255 and T265, which were identified in MD simulations as important for E-M coupling, but for which mutations still show functional currents (Fig. 3c). Residue V255 was found to be important for the AO state E-M coupling (Fig. 3). Each pair of residues is represented by a black dashed line connecting their respective sidechains.

a

	S1				S2

```
              S1                         S2
droKCNAS  AAIISVFVILLSIVIFCLETLPEFEDPFFLIETLCIIWFTFELTVRFLAC
pigKCNB1  AAIISIMFIVLSTIALSLNTLPELQPQLAHVEAVCIAWFTMEYLLRFLSS
ratKCNC1  AAFASLFFILVSITTFCLETHERFAAFLTYIEGVCVVWFTFEFLMRVVFC
bovKCND1  LYYVTGFFIAVSVIANVVETIPCRELAFFCMDTACVLIFTGEYLLRLFAA
mouKCNF1  AAVLSFLLILVSSVVMCMGTIPELDPTLENVETACIGWFTLEYLLRLFSS
chiKCNG2  GACISISFVAITAVSLCISTMPDVEYDIFVLETVCVAWFSFEFLLRSIQA
humKCNQ1  VHFAVFLIVLVCLIFSVLSTIEQYAGTLFWMEIVLVVFFGTEYVVRLWSA
orgKCNV1  AGVISIIFVVVSIINMALMSAELS-QLLEILEYVCISWFTGEFVLRFLCV
rabKCNS3  LAISSLSVVLASIVAMCVHSMSEFQPVLEGVEIACIAWFTGELAVRLVAA

              S3                         S4
droKCNAS  PNKLNFCRDVMNVIDIIAIIPYFITLAILRVIRLVRVFRIFKLSRHSKGL
pigKCNB1  PKKWKFFKGPLNAIDLLAILPYYVTIRVVQIFRIMRILRILKLARHSTGL
ratKCNC1  PNKVEFIKNSLNIIDFVAILPFYLEVGFLRVVRFVRILRIFKLTRHFVGL
bovKCND1  PSRCRFLRSVMSLIDVVAILPYYIGLGAFVTLRVFRVFRIFKFSRHSQGL
mouKCNF1  PNKLHFALSFMNIVDVLAILPFYVSLQAVQALRIMRIARIFKLARHSSGL
chiKCNG2  ENKCAFLKTPLNIIDILAILPFYISLLVLRFLRALRILYVMRLARHSLGL
humKCNQ1  GCRLRFARKPISIIDLIVVVASMVVLSAIRGIRFLQILRMLHVDRQGGTW
orgKCNV1  RDRCRFLRKVPNIIDLLAILPFYITLRIVQVLRLLRALRMLKLGRHSTGL
rabKCNS3  PCQKKFWKNPLNIIDFVSIIPFYATLKVVQILRLMRIFRILKLARHSVGL

       S4-S5L           S5                 Pore
droKCNAS  QILGRTLKASMRELGLLIFFFIGVVLFSSAVYFAGSENSFFKSIPDAFWW
pigKCNB1  QSLGFTLRRSYNELGLLILFAMGIMIFSSLVFFKDEDDTKFKSIPASFWW
ratKCNC1  RVLGHTLRASTNEFLLLIIFALGVLIFATMIAEPNDPSASFKNIPIGFWW
bovKCND1  RILGYTLKSCASELGFLLFSTMAIIIFATVMAEKGTNKTNFTSIPAAFWY
mouKCNF1  QTLTYALKRSFKELGLLLMYAVGIFVFSALGMEQSHPETLFKSIPQSFWW
chiKCNG2  QTLGLTVRRCTREFGLLLLFCVAMALFSPLVAEELGAKQEFTSIPTSYWW
humKCNQ1  RLLGSVVFIHRQELITTLYIGFLGLIFSSYFLANESGRVEFGSYADALWW
orgKCNV1  RSLGMTITQCYEEVGLLLLFSVGISIFSTV-YFQSIPDTTFTSVPCAWWW
rabKCNS3  RSLGATLRHSYHEVGLLLLFSVGISIFSVLIVEKDDHTSSLTSIPICWWW

         Pore                     S6
droKCNAS  AVVTMTTVGYGDMTPVGVWGKIVGSLCAIAGVLTIALPVPVIVSNFNYFT
pigKCNB1  ATITMTTVGYGDIYPKTLLGKIVGGLCCIAGVLVIALPIPIIVNNFSEFK
ratKCNC1  AVVTMTTLGYGDMYPQTWSGMLVGALCALAGVLTIAMPVPVIVNNFGMYL
bovKCND1  TIVTMTTLGYGDMVPSTIAGKIFGSICSLSGVLVIALPVPVIVSNFSRIQ
mouKCNF1  AIITMTTVGYGDIYPKTTLGKLNAAISFLCGVIAIALPIHPIINNFVRYQ
chiKCNG2  AVISMTTVGYGDMVPRSIPGQVVALSSILSGILLMAFFPVTSIFHTFSRSL
humKCNQ1  GVVTVTTIGYGDKVPQTWVGKTIASCFSVFAISFFALPAGILGSGFALKQ
orgKCNV1  ATTSMTTVGYGDIRPDTTTGKIVAFMCILSGILVLALPIAIINDRFSA-C
rabKCNS3  ATISMTTVGYGDTHPVTLAGKLIASTCIICGILVVALPITIIFNKFSKYK
```

b D_i (Conservation)

S1 S2 S3 S4 S4-S5L S5 Pore S6

Amino acid position

c Number — Eigenvalues

d IC1   IC2   IC3   IC4   IC5

Supplementary Fig. 7. Statistical coupling analysis of domain-swapped K$_V$ channels.

(a) Expanded sample MSA (from Figure 6a) used as input for analysis by SCA. MSA uses the nomenclature established by the HUGO Gene Nomenclature Committee (HGNC) for voltage-gated potassium channels[8]. K$_V$ channels can adopt two types of architectures. In "domain-swapped" channels, the VSD from one subunit contacts the PD from the neighboring subunit. In "non-domain-swapped" channels, the VSD from one subunit contacts the PD from the same subunit. These distinct architectures likely give rise to different modes of E-M coupling. SCA was applied to the K$_V$ channel superfamily previously[9]; however, prior studies utilized both domain-swapped and non-domain swapped K$_V$ channels in the input data. In this MSA, only domain-swapped K$_V$ channels were included. One member from each of K$_V$1 – K$_V$9 is shown. The final processed MSA includes 1421 sequences at 200 positions. **(b)** First order conservation by amino acid position within the MSA. D_i on the y-axis is calculated based on Kullback-Leibler divergence which measures deviation of the observed amino acid frequency in the MSA (Fig. 6a)

14

from the natural "background" amino acid frequency (see Methods). Bars indicate positions of the helical segments. **(c)** A histogram of eigenmodes tallied by their associated eigenvalues from SCA calculation (black). Red indicates the spectrum calculated by randomizing the input. Five significant eigenmodes can be seen by the black bars rising above the randomized red curve (blue arrows) at high eigenvalues. Inset shows enlarged scales. **(d)** Amino acid residues within independent component 1 through independent component 5 identified by SCA mapped onto the $K_V7.1$ cryoEM structure. Blue surfaces indicate all IC positions on one subunit, pink surfaces indicate the same IC positions on the neighboring subunit. Only the S5 and S6 helices are shown on the neighboring subunit for sake of clarity (pink helices). Accordingly, only the IC positions on the neighboring subunit on S5 and S6 are shown (pink surfaces). Using the IC submatrix and based on the strength of external correlation (see Methods, Figure 6c), IC2+IC3 are combined to form sector 1 (Fig. 6d), while IC1+IC4+IC5 are combined to form sector 2 (Fig. 6e). Source data for SCA are provided in Source Data file.

References

1. Hou, P. et al. Inactivation of KCNQ1 potassium channels reveals dynamic coupling between voltage sensing and pore opening. *Nat Commun* **8**, 1730 (2017).
2. Hou, P., Shi, J., White, K. M., Gao, Y. & Cui, J. ML277 specifically enhances the fully activated open state of KCNQ1 by modulating VSD-pore coupling. *Elife* **8** (2019).
3. Zaydman, M. A. et al. Domain-domain interactions determine the gating, permeation, pharmacology, and subunit modulation of the IKs ion channel. *Elife* **3**, e03606 (2014).
4. Wu, D., Pan, H., Delaloye, K. & Cui, J. KCNE1 remodels the voltage sensor of Kv7.1 to modulate channel function. *Biophys J* **99**, 3599-608 (2010).
5. Xu, Y. et al. Building KCNQ1/KCNE1 channel models and probing their interactions by molecular-dynamics simulations. *Biophys J* **105**, 2461-73 (2013).
6. Nakajo, K. & Kubo, Y. Steric hindrance between S4 and S5 of the KCNQ1/KCNE1 channel hampers pore opening. *Nat Commun* **5**, 4100 (2014).
7. Choveau, F. S. et al. KCNQ1 channels voltage dependence through a voltage-dependent binding of the S4-S5 linker to the pore domain. *J Biol Chem* **286**, 707-16 (2011).
8. Gutman, G. A. et al. International Union of Pharmacology. LIII. Nomenclature and molecular relationships of voltage-gated potassium channels. *Pharmacol Rev* **57**, 473-508 (2005).
9. Lee, S. Y., Banerjee, A. & MacKinnon, R. Two separate interfaces between the voltage sensor and pore are required for the function of voltage-dependent K(+) channels. *PLoS Biol* **7**, e47 (2009).